DOI 10.5162/iCCC2024/2.3

Contactless Assessment of Physiological Parameters with a 61 GHz CW Medical Radar System

Robert Holzschuh, Thiem-Research GmbH, Cottbus, Germany, r.holzschuh@ctk.de
Hui Lu, Brandenburgische Technische Universität Cottbus-Senftenberg, Cottbus, Germany, hui.lu@tuhh.de
Batuhan Sutbas, IHP – Leibniz-Institut für innovative Mikroelektronik, Frankfurt (Oder), Germany, suetbas@ihp-microelectronics.com
Ayse Ecem Bezer, Fraunhofer IZM, Cottbus, Germany, ayse.ecem.bezer@izm.fraunhofer.de
Robert Freund, Thiem-Research GmbH, Cottbus, Germany, r.freund@ctk.de
Steffen Ortmann, Thiem-Research GmbH, Cottbus, Germany, s.ortmann@ctk.de
Dirk Große Meininghaus, Carl-Thiem-Klinikum, Cottbus, Germany, d.grosse-meininghaus@ctk.de

Summary:

1. Background
Implementation of sensor technology and analysis supported by artificial intelligence (AI) are important drivers of medical research in the healthcare sector. Studies demonstrate the reliability, robustness, and efficiency of existing systems and illustrate synergistic benefits of clinical expertise, sensor technology and AI.

2. Technical Description and Use
This study uses a high-frequency 61 GHz continuous-wave (CW) radar system for contactless detection of cardiorespiratory parameters. The newly developed radar system offers unique advantages including higher level of integration, improved sensitivity, and smaller size compared to systems operating at lower frequencies. Respiration and heart beat rates are key parameters in the monitoring of physiologic and pathologic settings. Thus, the proposed approach may improve quality of medical care in hospitals. In addition, and in contrast to conventional monitoring based on electrodes and registration-lines, patient comfort is increased and applicability for the clinical staff is improved. The proposed radar system incorporates three stacked boards including frontend, baseband, and microcontroller components. The frontend board has a 30.5 GHz voltage-controlled oscillator (VCO) chip integrated with a divide-by-16 chain that is stabilized in a phase-locked loop (PLL) and a 61 GHz transceiver (TRX) chip equipped with an in-phase/quadrature (I/Q) receiver. Both VCO and TRX chips have been designed and fabricated in an advanced silicon-germanium (SiGe) BiCMOS technology. Intermediate frequency (IF) outputs are dc-coupled to enable CW measurements of the low frequency spectrum of physiologic parameters. A series-fed 2×8 patch antenna array on the frontend board is equipped on a 254-µm-thick Megtron6 substrate with a gain of 12.7 dB and an RF bandwidth of 5.1 GHz (range 57.5 to 62.6 GHz). The array has a beamwidth of 15° E-plane and 50° H-plane, and a simulated radiation efficiency of 72%. A wideband planar RF balun is developed at 61 GHz to interface the single-ended antenna array input with the differential transmitter and receiver outputs of the TRX chip. The integration of 61 GHz TRX with the balun is achieved by 25-µm-diameter gold bondwires.

3. Post-Processing
The raw IF data output is digitized by a baseband board and transferred to a computer by an STM32 microcontroller evaluation board. Raw radar I/Q signals are band-pass filtered and transformed in pulse-wave and heart sound signals. Based on earlier datasets, a deep learning model was pre-trained and applied for the analysis of the heart beat and the beat-to-beat-interval (IBI) out of the filtered signals. Initial results comparing the accuracy of the radar system to a conventional electrocardiogram (ECG) recorder show a high F1 score up to 0.99 for heart beat detection. In addition, effects of patient movement, e.g., random- and speaking associated movements, and body-position are part of the presented study.

Keywords: CW radar, vital signs detection, beat-to-beat interval, heart rate, respiration rate

1 Introduction

Monitoring of cardiorespiratory parameters is key for patient surveillance and detection of otherwise unnoticed deterioration. Conventional methods using adhesive electrodes or wearable sensors have limitations in terms of complexity and patient discomfort. In contrast, non-contact radar detection technology emerges as a user-friendly alternative, eliminating the need for electrodes, thus enabling monitoring at distance. Various radar systems, e.g., continuous-wave (CW), doppler radar [1, 2], ultra-wideband (UWB) impulse radar [3, 4], and frequency-modulated CW (FMCW) doppler radar [5, 6] are commonly used. Multiple-input-multiple-output (MIMO) antenna systems allow the localization of multiple moving targets. Radar sensors are capable to detect tiny movements of the patient body surface, thus identifying both breathing and heart beat. In this work, a high-frequency 61 GHz CW radar system with unique features is reported, e.g., improved integration, enhanced sensitivity, and reduced size compared to lower-frequency systems. In addition, initial clinical results are described.

2 Methods

Technical architecture of the radar system with the post-processing and signal analysis method for detection of cardiorespiratory parameter is explained in this section. In addition, the setup for clinical feasibility analysis is presented.

2.1 Radar System Design

The radar system, shown in Figure 1, has three stacked boards: the radar frontend, including the integrated circuits and antenna, the baseband and the interface board.

Fig. 1. Radar system in housing.

2.1.1 Integrated Circuit Design

The 30.5 GHz voltage-controlled oscillator (VCO) and 61 GHz transceiver (TRX) integrated circuits are manufactured in the mature 130-nm SiGe BiCMOS process at IHP, SG13S, with fT and fmax of 250 GHz and 330 GHz, respectively. Both chips share a single supply of 3.3 V. The micrographs of the bonded chips on the frontend board are shown in Figure 2.

The fully-differential TRX chip [7] utilizes a Gilbert-based frequency doubler to scale the local oscillator (LO) signal from the VCO. The chip consumes 0.6 W of dc power and occupies a silicon area of 1.74 × 2.14 mm2. The high saturated transmit output power of 11.5 dBm and receiver gain of 24 dB enable detection of reflected signals from human body surface. On-chip modulators are bypassed to enable the CW mode. The dc-coupled in-phase/quadrature (I/Q) receiver network allows the detection of low-frequency vital signals and the quadrature phase demodulation. Furthermore, the LO scalable architecture of the TRX chip facilitates a daisy chain cascade for further MIMO implementations.

The Colpitts-based VCO chip [7] utilizes a fully-differential topology as well. The chip including a divide-by-16 signal chain and output buffer stages consumes in average 230 mW of dc power and occupies a silicon area of 0.94 × 0.94 mm2. The wide tuning range exceeding 2.5 GHz ensures radar operation in the predefined ISM-band. The low phase noise of the VCO is −106 dBc/Hz at an offset frequency of 1 MHz in combination with the phase-locked loop (PLL) chip ADF4158 allows high precision measurement in the overall system.

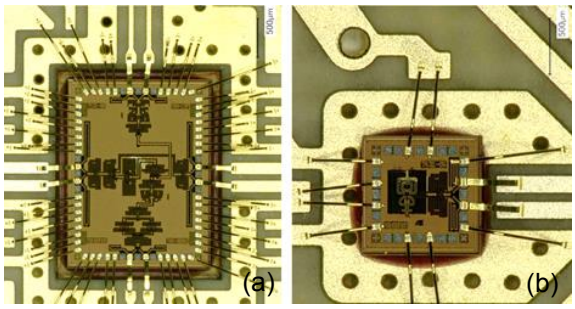

Fig. 2. Micrographs of the fabricated and bonded ICs: (a) TRX and (b) VCO.

2.1.2 Antenna Array Design

A series-fed 2×8 patch antenna array is designed on a 254-µm Megtron6 substrate. Permittivity and loss tangent of the substrate are given as 3.62 and 0.006 at 60 GHz, respectively. Gain of the 2×8 array including the balun at the input is 12.7 dB. RF bandwidth of the antenna ranges from 57.5 GHz to 62.6 GHz. The 2×8 array has a beamwidth of 15° in E-plane and 50° in H-plane. Simulated radiation efficiency is 72%. Uniformity of the array provides high side lobe levels (SLL). The left and right SLL are −10 dB and −8.6 dB, respectively.

Figure 3 shows the simulation model and final fabrication of the 2×8 antenna array.

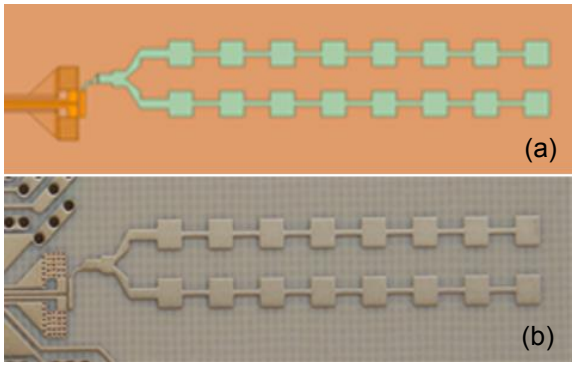

Fig. 3. 2×8 patch antenna array with differential to single-ended balun at the input: (a) simulation model and (b) fabricated on frontend board.

To prevent direct coupling of transmitter (Tx) and receiver (Rx) antennas, they are placed at the opposite sides of the TRX chip, achieving isolation exceeding 70 dB. The wideband planar RF balun at 61 GHz is essential to connect the single-ended antenna array input to the differential output of the transceiver chip. The final integration of 61 GHz TRX with the balun is achieved by 25-µm-diameter gold bondwires. Table 1 shows the 2×8 antenna array specifications.

Tab. 1: Specifications of the 2×8 patch antenna array

Reflection coef. at ISM band	−21 dB
−10 dB RF bandwidth	57.5 to 62.6 GHz
Max. realized gain	12.7 dB
Radiation efficiency	72 %
E-plane HPBW	14.6 °
H-plane HPBW	50 °
Left SLL	−10 dB
Right SLL	−8.6 dB
Tx-Rx antenna coupling coef.	−71.2 dB

2.1.3 Baseband Board Design

The baseband board is the interface between the frontend and microcontroller evaluation boards. The board includes the voltage regulation, operational amplification and data conversion circuits. The sampled raw data from the frontend board are digitized and sent to the microcontroller board.

2.1.4 Post-Processing and Signal Analysis

The method of heart beat detection is described elsewhere [8]. In summary, the radar in-phase (I) and quadrature (Q) signals are filtered directly in heart sound (HS) and pulse wave frequency ranges by a fourth-order Butterworth filter [9]. Thereafter, the filtered heart sound and pulse waves I/Q signals are transmitted to a bi-directional gated recurrent unit (bi-GRU), and outputs from the bi-GRU are fused to generate the heart beat sequence. The model is trained with data previously acquired from a 24 GHz CW radar system and directly applied to our data collected from the 61 GHz CW radar. Two respiration rate extraction methods are compared. On the one hand, Complex Signal Decomposition (CSD) [10] applies fast Fourier transformation (FFT) to the complex I/Q signals to generate the spectrum. On the other hand, extraction of the distance signals by Arctangent Demodulation (AD) and FFT of the distance signals is performed. The respiration rate is extracted as peak of the spectrum in the frequency range of 0.1 to 0.5 Hz, corresponding to 6 to 30 breathing cycles per minute (BrPM).

2.2 Clinical Measurement Setup

To perform a clinical feasibility analysis of the measurement of vital parameters, the radar system was mounted under the lattice of a hospital bed. This arrangement ensured a consistent distance of approximately 10 cm from the radar to the back of the test person. For reference, the radar system underwent synchronization with the medically approved standard device (BioPac MP160) equipped with a three-channel electrocardiogram (ECG) and a respiration belt. The latter allowed continuous measurement of heart rate and respiration rate, thus providing a reliable baseline to evaluate the accuracy of the radar system. At start, cardiorespiratory parameters were collected in a supine position (37 minutes), followed by a 5-minute period with loud reading of a given text. Thereafter, parameters were recorded in left- and right-sided body positions and in prone position for five minutes, each. These varying scenarios were documented to assess a comprehensive range of data.

3 Initial Results

Figure 4 illustrates the measured data and prediction model in a 5 s period. The black dashed line indicates the R peaks detected by ECG-reference, showing the position of each heart beat. The red line shows the prediction probability of the pre-trained model. The peaks from the prediction align with the R peaks, indicating that all heart beats are detected correctly. The beat-to-beat-interval (IBI) based metrics include root mean square error (RMSE) and the calculated correlation of ECG and radar. Table 1 summarizes the performance results in different scenarios for a test person. In the scenarios supine, left-sided, and prone position, heart beat detection demonstrates an F1 exceeding 0.96. However, in right-sided position, F1 is lower, indicating an impaired heart sound quality in this position.

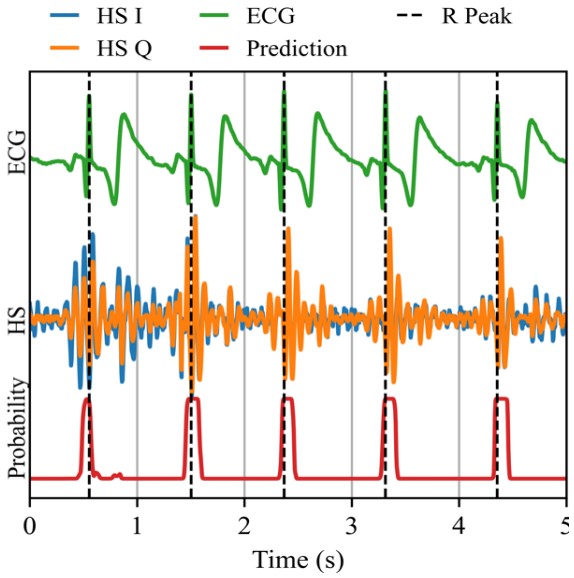

Fig. 4. Example of the prediction result.

The scenario with loud reading shows suboptimal results due to distortion of the radar signals. In comparison to the other scenarios, the supine scenario is outstanding with the lowest RMSE of 18.95 ms, indicating minimal IBI measurement error, and the highest correlation value of 0.968, underlining strong data consistency between IBI from radar and ECG.

Tab. 1: Performance metrics in different scenarios.

Scenario	Prec	Sens	F1	RMSE (ms)	Correlation
Back	0.99	0.99	0.99	18.95	0.968
Reading	0.52	0.53	0.53	160.25	0.053
Left side	0.96	0.97	0.96	63.61	0.646
Right side	0.88	0.85	0.86	101.50	0.370
Abdominal	0.98	0.97	0.97	30.78	0.899

The average respiration rate error is reported in Table 2. With AD, the respiration rate error was smaller than 2 BrPM except for the registration during reading. With the CSD method, a slightly higher error values was calculated for reading, for the left-sided and right-sided scenarios compared to AD. For the remaining scenarios both methods achieved similar performance results for estimation of respiration.

Tab. 2: Absolute respiration rate error with CSD and AD.

Scenario	CSD (BrPM)	AD (BrPM)
Back	1.27	1.46
Reading	3.27	2.73
Left side	2.20	1.60
Right side	1.82	1.46
Abdominal	1.77	1.77
Sum	1.64	1.63

4 Discussion

The potential applications of non-contact radar detection technology are diverse, covering continuous monitoring of newborns, patients with burns, epilepsy, in psychiatric care, but also for mobile patients. Additionally, this technology reduces the burden of medical staff and offers long-term cost reduction in patient monitoring. The integration of sensor technology and artificial intelligence is crucial to push medical research in healthcare. Ongoing studies emphasize the reliability and efficiency of available systems, showcasing their potential to improve healthcare practice [11]. This symbiotic relationship between clinical expertise, sensor technology, and AI gives rise to a new era of interdisciplinary collaboration [12]. In addition, sensor technology offers a wide range of applications in home environment, e.g., sleep monitoring of infants. Furthermore, the increasing demand of people to monitor their health data by digital sensor applications, in detail cardiopulmonary data, may contribute to early detection of respiratory or cardiovascular diseases, still the most common cause of death worldwide [13]. By demonstration of the functionality of the presented method in combination with the benefits of a non-invasive application, the proposed approach might pave the way for routine use of radar systems in healthcare. In addition, the radar data may be used for calculation of heart rate variability and detection of arrhythmia if supported by artificial neural networks.
Although the measurement of cardiorespiratory parameters by the radar system could be demonstrated, we are not able to provide a statistical evaluation so far. A clinical study with this radar system in the Department of Cardiology at Carl-Thiem-Klinikum is ongoing to collect more data for analysis.

5 Conclusions

These initial results show that the presented radar system is capable of accurate measurement of heart rate, IBI and respiration at least under discrete conditions. However, further data in a clinical study are urgently needed to draw conclusions for clinical scenarios.

6 Acknowledgement

The research project iCampµs Cottbus is supported by the Federal Ministry of Education and Research (BMBF), Berlin, Germany, project grant No. 16ME0421.

7 Literature

[1] Lv Q, Chen L, An K, Wang J, Li H, Ye D, Huangfu J, Li C, Ran L., Doppler Vital Signs Detection in the Presence of Large-Scale Random Body Movements. IEEE Trans. Microw. Theory Tech.

2018;66:4261-70. doi: 10.1109/TMTT.2018.2852625.

[2] Malešević N, Petrović V, Belić M, Antfolk C, Mihajlović V, Janković M., Contactless Real-Time Heartbeat Detection via 24 GHz Continuous-Wave Doppler Radar Using Artificial Neural Networks. Sensors (Basel). 2020 Apr 21;20(8):2351. doi: 10.3390/s20082351. PMID: 32326190; PMCID: PMC7219229.

[3] Schires E, Georgiou P, Lande TS. Vital Sign Monitoring Through the Back Using an UWB Impulse Radar With Body Coupled Antennas. IEEE Trans Biomed Circuits Syst. 2018 Apr;12(2):292-302. doi: 10.1109/TBCAS.2018.2799322. PMID: 29570057.

[4] Lee Y, Park JY, Choi YW, Park HK, Cho SH, Cho SH, Lim YH. A Novel Non-contact Heart Rate Monitor Using Impulse-Radio Ultra-Wideband (IR-UWB) Radar Technology. Sci Rep. 2018 Aug 29;8(1):13053. doi: 10.1038/s41598-018-31411-8. PMID: 30158545; PMCID: PMC6115337.

[5] Iyer S, Zhao L, Mohan MP, Jimeno J, Siyal MY, Alphones A, Karim MF. mm-Wave Radar-Based Vital Signs Monitoring and Arrhythmia Detection Using Machine Learning. Sensors (Basel). 2022 Apr 19;22(9):3106. doi: 10.3390/s22093106 PMID: 35590796; PMCID: PMC9104941.

[6] Xiang M, Ren W, Li W, Xue Z, Jiang X, High-Precision Vital Signs Monitoring Method Using a FMCW Millimeter-Wave Sensor. Sensors (Basel). 2022 Oct 5;22(19):7543. doi: 10.3390/s22197543. PMID: 36236641; PMCID: PMC9572116.

[7] H. J. Ng, M. Kucharski, W. Ahmad and D. Kissinger, "Multi-Purpose Fully Differential 61- and 122-GHz Radar Transceivers for Scalable MIMO Sensor Platforms," in *IEEE Journal of Solid-State Circuits*, vol. 52, no. 9, pp. 2242-2255, Sept. 2017.

[8] Lu, H., Heyder, M., Wenzel, M., Albrecht, N. C., Langer, D., & Koelpin, A. (2023, January), Accurate Heart Beat Detection with Doppler Radar using Bidirectional GRU Network. In 2023 IEEE Radio and Wireless Symposium (RWS) (pp. 52-54). IEEE.

[9] S. Schellenberger, K. Shi, T. Steigleder, A. Malessa, F. Michler, L. Hameyer, N. Neumann, F. Lurz, R. Weigel, C. Ostgathe et al., "A dataset of clinically recorded radar vital signs with synchronised reference sensor signals", Sci. Data, vol. 7, no. 1, pp. 1-11, 2020.

[10] C. Li and J. Lin, “Random body movement cancellation in doppler radar vital sign detection,” IEEE Transactions on Microwave Theory and Techniques, vol. 56, no. 12, pp. 3143–3152, 2008.

[11] Yu KH, Beam AL, Kohane IS, Artificial intelligence in healthcare. Nat Biomed Eng. 2018 Oct;2(10):719-731. doi: 10.1038/s41551-018-0305-z. Epub 2018 Oct 10. PMID: 31015651.

[12] Manickam P, Mariappan SA, Murugesan SM, Hansda S, Kaushik A, Shinde R, Thipperudraswamy SP, Artificial Intelligence (AI) and Internet of Medical Things (IoMT) Assisted Biomedical Systems for Intelligent Healthcare. Biosensors (Basel). 2022 Jul 25;12(8):562. doi: 10.3390/bios12080562. PMID: 35892459; PMCID: PMC9330886.

[13] Prabhakaran D, Anand S, Watkins D, Gaziano T, Wu Y, Mbanya JC, Cardiovascular, respiratory, and related disorders: key messages from Disease Control Priorities, 3rd edition. Lancet. 2018 Mar 24;391(10126):1224-36. doi: 10.1016/S0140-6736(17)32471-6. PMID: 29108723; PMCID: PMC5996970.